Articles in PresS. Am J Physiol Endocrinol Metab (November 18, 2014). doi:10.1152/ajpendo.00472.2014

Spermine Oxidase Maintains Basal Skeletal Muscle Gene Expression and Fiber Size, and Is Strongly Repressed by Conditions that Cause Skeletal Muscle Atrophy*

Kale S. Bongers[#,1], Daniel K. Fox[#,1], Steven D. Kunkel[1], Larissa V. Stebounova[2], Daryl J. Murry[2], Miles A. Pufall[3], Scott M. Ebert[1], Michael C. Dyle[1], Steven A. Bullard[1,4], Jason M. Dierdorff[1], and Christopher M. Adams[1,4]

[1]From the Departments of Internal Medicine and Molecular Physiology and Biophysics and Fraternal Order of Eagles Diabetes Research Center, Roy J. and Lucille A. Carver College of Medicine, [2]the College of Pharmacy, and [3]the Department of Biochemistry, Roy J. and Lucille A. Carver College of Medicine, The University of Iowa, Iowa City, Iowa 52242, [4]Iowa City Veterans Affairs Medical Center, Iowa City, IA 52246, USA

[#]Authors contributed equally to this work.

Running title: Role of Spermine Oxidase in Skeletal Muscle Atrophy

*Address correspondence: Christopher M. Adams

Phone: (319) 353-5786. E-mail: christopher-adams@uiowa.edu

ABSTRACT

Skeletal muscle atrophy is a common and debilitating condition that remains poorly understood at the molecular level. To better understand the mechanisms of muscle atrophy, we used mouse models to search for a skeletal muscle protein that helps to maintain muscle mass and is specifically lost during muscle atrophy. We discovered that diverse causes of muscle atrophy (limb immobilization, fasting, muscle denervation, and aging) strongly reduced expression of the enzyme spermine oxidase. Importantly, a reduction in spermine oxidase was sufficient to induce muscle fiber atrophy. Conversely, forced expression of spermine oxidase increased muscle fiber size in multiple models of muscle atrophy (immobilization, fasting, and denervation). Interestingly, the reduction of spermine oxidase during muscle atrophy was mediated by p21, a protein that is highly induced during muscle atrophy and actively promotes muscle atrophy. In addition, we found that spermine oxidase decreased skeletal muscle mRNAs that promote muscle atrophy (e.g. *myogenin*) and increased mRNAs that help to maintain muscle mass (e.g. *mitofusin-2*). Thus, in healthy skeletal muscle, a relatively low level of p21 permits expression of spermine oxidase, which helps to maintain basal muscle gene expression and fiber size; and conversely, during conditions that cause muscle atrophy, p21 expression rises, leading to reduced spermine oxidase expression, disruption of basal muscle gene expression, and muscle fiber atrophy. Collectively, these results identify spermine oxidase as an important positive regulator of muscle gene expression and fiber size, and elucidate p21-mediated repression of spermine oxidase as a key step in the pathogenesis of skeletal muscle atrophy.

INTRODUCTION

Skeletal muscle atrophy is a major clinical disorder that is caused by a variety of conditions including immobilization, starvation, muscle denervation, aging, and severe illness. In addition to being very prevalent, muscle atrophy has serious consequences, including weakness, fatigue, reduced quality of life, falls, fractures, delayed recovery from acute illness, loss of independent living, and increased mortality (4, 18, 25, 46). Although the clinical implications of muscle atrophy are broad, a pharmacologic therapy does not exist. Furthermore, therapeutic advances are hindered by the fact that muscle atrophy remains poorly understood at the molecular level.

Some insight into the molecular mechanisms of muscle atrophy has been gained through investigations of mRNA expression changes that occur in atrophying skeletal muscle. Through a complex network of signaling pathways, primary causes of muscle atrophy generate new patterns of mRNA expression in skeletal muscle (1, 5, 16, 19, 20, 22, 24, 30, 39, 44, 48, 49). These patterns, or signatures, consist of mRNAs that are expressed at relatively low levels in healthy skeletal muscle, but are significantly increased by conditions that cause muscle atrophy; and also mRNAs that are expressed at relatively high levels in healthy skeletal muscle, but are significantly decreased by conditions that cause muscle atrophy. Because mRNA expression signatures of muscle atrophy are highly specific and crucial for atrophy, they can be used to identify pharmacologic approaches that attenuate muscle atrophy (13, 24), as well as proteins that play key roles in the pathogenesis of muscle atrophy. For example, investigations focused on certain mRNAs that are strongly induced in atrophying muscle have identified proteins that actively promote muscle atrophy, including key transcriptional regulators and proteins involved in ubiquitin-mediated proteolysis and autophagy (5, 6, 14, 15, 17, 21, 23, 32, 33, 35). Conversely, mRNAs that are strongly repressed in atrophic muscle encode proteins that promote mitochondrial function and other cellular processes that help to maintain skeletal muscle mass, but are impaired during muscle atrophy (10, 11, 27, 40, 50).

Despite these advances, the vast majority of skeletal muscle mRNAs whose levels are significantly altered during muscle atrophy remain unstudied. On this basis, we hypothesized that critical regulators of skeletal muscle mass remain to be discovered. Thus, in the current study, we sought to identify a positive regulator of muscle mass and a previously unrecognized mechanism of muscle atrophy by identifying and investigating an mRNA transcript that is strongly and specifically repressed in atrophic skeletal muscle.

MATERIALS AND METHODS

Chemicals and Antibodies

We obtained HPLC-grade spermine, spermidine, methanol, and acetonitrile from Sigma; N,N′-Bis(3-aminopropyl)-1,4-butane-d_{20}-diamine (deuterated spermine) from C/D/N Isotopes; HPLC-grade heptafluorobutyric acid (HFBA) and formic acid from Thermo Scientific; and ammonium hydroxide (ACS grade, 28-30%) from VWR International. Rabbit polyclonal anti-spermine oxidase antibody (#15052-1-AP) was obtained from Proteintech. Mouse monoclonal anti-p21 antibody (SC-6246) was obtained from Santa Cruz Biotechnology. Mouse monoclonal anti-FLAG antibody (#F1804) was obtained from Sigma. Mouse monoclonal anti-mitofusin-2 antibody (ab56889) was obtained from Abcam. Mouse monoclonal anti-myogenin antibody (F5D) was obtained from the Developmental Studies Hybridoma Bank at the University of Iowa.

Mouse Protocols

Male C57BL/6 mice were obtained from the National Cancer Institute at 6-8 weeks of age, or from the National Institute on Aging at 22 months of age. Mice were housed in colony cages at 21 °C with 12 h light/12 h dark cycles and provided *ad libitum* access to standard chow (Harlan Teklad 7013) except during fasting experiments. The protocols for limb immobilization, fasting, muscle denervation, and *in vivo* transfection of plasmid DNA into mouse skeletal muscle were described previously (6, 14, 15). Briefly, in the limb immobilization protocol, mice were anesthetized and an Autosuture Royal 35W skinstapler (Tyco Healthcare) was used to immobilize one ankle joint and tibialis anterior (TA) muscle in each mouse (7). In the fasting protocol, food but not water was removed from mice for 24 h. In the denervation protocol, mice were anesthetized and then one sciatic nerve in each mouse was transected near the head of the femur. All experiments utilized TA muscles with the exception of the experiments in Figs. 2*H* and 2*I,* which utilized quadriceps muscles. All animal protocols were approved by the Institutional Animal Care and Use Committee of the University of Iowa.

Genome-Wide mRNA Expression Arrays

Skeletal muscle RNA was extracted with TRIzol (Invitrogen) and purified with an RNeasy kit and RNase-free DNase set (Qiagen). RNA was processed and hybridized to Mouse Ref-8 v2.0 BeadChip arrays (Illumina) by the Southern California Genotyping Consortium (University of California, Los Angeles) as described previously (17). Following hybridization, arrays were washed, blocked, stained, and dried (Little Dipper processor). Arrays were scanned with an iScan reader and data were extracted and analyzed with BeadStudio Software (Illumina). The array data have been deposited in the NCBI Gene Expression Omnibus (GEO) under the accession number GSE63008.

Quantitative Real-time RT-PCR

Harvested mouse skeletal muscles were immediately incubated in RNAlater (Ambion), and then RNA was extracted with TRIzol (Invitrogen) and treated with DNase (Turbo DNA-*free* kit, Ambion) as described previously (6). First-strand cDNA was synthesized in a 20 μl reaction containing 2 μg RNA, random hexamer primers, RNase inhibitor, and components of the High-Capacity cDNA reverse transcription kit (Applied Biosystems). All quantitative RT-PCR was performed on a 7900HT Fast Real-time PCR System (Applied Biosystems) using Taqman Gene Expression Assays (Applied Biosystems) for *spermine oxidase*, *p21, Myog, and Mfn2*. *36B4* was used as the invariant control. Samples were run in triplicate, cycle threshold (C_t) values were averaged, and the $\Delta\Delta C_t$ method was used to calculate fold changes.

Immunoblot Analysis

Harvested mouse skeletal muscles were snap-frozen in liquid nitrogen and homogenized in 1 ml ice-cold homogenization buffer (50 mM HEPES, 4 mM EGTA, 10 mM EDTA, 15 mM sodium pyrophosphate, 100 mM β-glycerophosphate, cOmplete Mini protease inhibitor mixture (Roche Applied Science), 25 mM sodium fluoride, 1% (vol/vol) Triton X-100, and a 1:100 dilution of phosphatase inhibitor cocktails 2 and 3 (Sigma) (6)); using a Tissue Master 240 (Omni International) for 1 min on setting #10. The

homogenate was rotated for 1 h at 4°C and then centrifuged at 16,000 x *g* for 20 min at 4°C. An aliquot of the supernatant was used to determine protein concentration by the BCA method, and another aliquot of supernatant was mixed with 0.25 volume of sample buffer (250 mM Tris HCl, pH 6.8, 10% SDS, 25% glycerol, 0.2% (wt/vol) bromophenol blue, and 5% (wt/vol) 2-mercaptoethanol) and heated at 95°C for 5 min. An equal amount of protein from each muscle sample was subjected to SDS-PAGE and then transferred to Hybond-C extra nitrocellulose membranes (Millipore). Immunoblots were performed for 16 h at 4°C using a 1:2,000 dilution of anti-spermine oxidase antibody (used to detect endogenous and overexpressed spermine oxidase), a 1:1,000 dilution of anti-p21 antibody (used to detect endogenous and overexpressed p21 in Figure 6), a 1:3,000 anti-FLAG antibody (used to detect overexpressed p21 in Figure 7), a 1:1,000 dilution of anti-mitofusin-2 antibody (used to detect endogenous mitofusin-2), or a 1:500 dilution of anti-myogenin antibody (used to detect endogenous myogenin). Membranes were stained with Ponceau S to ensure equal loading.

Measurement of Skeletal Muscle Spermine and Spermidine Levels

Stock solutions of spermine and spermidine were prepared by dissolving spermine and spermidine in a water:methanol (80:20 vol/vol) solution at a concentration of 1 mg/ml. Working standards were prepared by combining 10 µl of each stock solution with 980 µl of water:methanol (to form a working standard containing 10 µg/ml spermine and 10 µg/ml spermidine), followed by serial dilution of this working standard in water:methanol (to form less concentrated working standards containing 1 µg/ml spermine and spermidine and 100 ng/ml spermine and spermidine). The internal standard was prepared by dissolving deuterated spermine in water:methanol at a concentration of 10 µg/ml. All solutions were stored at 4°C and brought to 21°C before use.

To generate blank samples, calibration standards, and positive controls, 400 mg of skeletal muscle from control mice were homogenized in 3.2 ml of ultrapure water, then centrifuged at 10,000 rpm for 5 min. Calibration standards and positive controls were prepared by spiking 200 µl homogenate with working

153 standards at 10, 50, 500, 1000, and 2000 ng/ml of spermine and spermidine (calibration standards) and
154 100 and 800 ng/ml (positive controls). We then added 10 µl of internal standard and 600 µl ammonium
155 hydroxide (1% wt/vol water) to each blank, calibration standard, and positive control. To prepare
156 experimental samples, mouse skeletal muscles were harvested under conditions described in the figure
157 legends, weighed, homogenized at high speed for 15 sec in 300 µl ultrapure water, and centrifuged at
158 10,000 rpm for 5 min. We then transferred 200 µl of homogenate to a fresh vial, and added 10 µl of
159 internal standard and 600 µl 1% ammonium hydroxide. Agilent BondElut-PSA solid phase extraction
160 cartridges (#12102015) were used for sample extraction on a Cerex SPE processor (Varian). Cartridges
161 were conditioned with methanol and equilibrated with 1% ammonium hydroxide in water. Samples were
162 then loaded into cartridges using nitrogen flow at a rate of 1 ml/min. The cartridges were rinsed with 1%
163 ammonium hydroxide in water and the analytes were eluted with 1% ammonium hydroxide in methanol.
164 Eluates were dried under flowing nitrogen at 35°C for 35 min. The residue was reconstituted with 320 µl
165 of 0.1% formic acid and 0.02% HFBA in ultrapure water (Mobile A) and 80 µl of 0.1% formic acid and
166 0.02% HFBA in acetonitrile (Mobile B).
167
168 Liquid chromatography separation was performed on a Shimadzu 2010A high performance liquid
169 chromatography mass spectrometry (HPLC–MS) system using electrospray ionization mode and
170 operating LC-MS Solution software (Version 2.04H3, Shimadzu). A Poroshell 120 SB-C18 analytical
171 column (Agilent) protected by a high pressure column pre-filter and a Phenomenex C-18 ultra HPLC
172 security guard column (#AJ0-8768) was held at 40°C. Chromatographic separation was done by gradient
173 elution using aqueous Mobile A and organic Mobile B. The gradient elution started with 10% Mobile B,
174 which increased to 50% at 6 min; the column was then rinsed at 90% Mobile B for 1 min and the system
175 was equilibrated back to 10% Mobile B for 4 min. The analytes were eluted at the retention times of 3.9
176 min (spermidine) and 4.6 min (spermine and deuterated spermine) using 0.25 ml/min flow rate and a 5 µl
177 injection volume. The mass spectrometer was tuned using a polyethylene glycol solution following
178 manufacturer's protocol. The electrospray source was operated in positive mode; the CDL and heat block

were heated to 250°C, nitrogen flow rate was 1.5 l/min and detector voltage was 1.6 kV. Nitrogen gas at 14.5 psi was flowing in the ionization chamber. The scan interval was 0.3 sec. Positive ions were monitored at *m/z* 146.15 for spermidine, *m/z* 203.25 for spermine, and *m/z* 223.4 for deuterated spermine.

Plasmids

p-Spermine Oxidase encodes the mu isoform of spermine oxidase with three copies of the FLAG epitope tag at the NH_3-terminus, under control of the cytomegalovirus (CMV) promoter. To generate *p-Spermine Oxidase*, we obtained a full-length mouse *spermine oxidase* cDNA from Genscript (Clone ID F16960), and then subcloned the cDNA into the *p3XFLAG-CMV10* vector (Sigma). *p-Spermine oxidase(H82E/T558Y)* encodes the mu isoform of spermine oxidase with two point mutations (H82E and T558Y) that disrupt spermine oxidase activity (47), and was generated by site-directed mutagenesis of *p-Spermine Oxidase*. *p-eGFP* encodes enhanced green fluorescent protein (eGFP) under control of the CMV promoter. *p-miR-Control* was described previously (14) and encodes emerald green fluorescent protein (EmGFP) and a nontargeting pre-miRNA under bicistronic control of the CMV promoter in the *pcDNA6.2GW/EmGFP-miR* plasmid (Invitrogen). *p-miR-Spermine Oxidase #1* and *p-miR-Spermine Oxidase #2* encode EmGFP and artificial pre-miRNAs targeting mouse spermine oxidase under bicistronic control of the CMV promoter, and were generated by ligating Mmi528584 and Mmi528586 oligonucleotide duplexes (Invitrogen), respectively, into the *pcDNA6.2GW/EmGFP-miR* plasmid. *p-p21* has been described previously (17) and encodes mouse p21 with three copies of the FLAG epitope tag at the NH_3-terminus, under control of the CMV promoter. *p-miR-p21* was described previously (as "*p-miR-p21 #1"* in (17)) and encodes EmGFP and an artificial pre-miRNA targeting mouse p21 under bicistronic control of the CMV promoter in the *pcDNA6.2GW/EmGFP-miR* plasmid.

Histological Analysis of Mouse Skeletal Muscle

Harvested muscles were immediately fixed in 4% (wt/vol) paraformaldehyde for 16 h at 4°C, and then incubated in 30% sucrose (wt/vol) for 24 h. The muscles were then embedded in Tissue Freezing

Medium (Triangle Biomedical Sciences), and a Microm HM 505E cryostat was used to prepare 10-μm sections from the muscle mid-belly. Sections were washed with PBS three times, mounted with Vectashield (Vector Laboratories), and then imaged on an Olympus IX-71 microscope equipped with a DP-70 camera. Images were analyzed with ImageJ, and transfected fibers were defined as fibers with a mean fluorescence of ≥ 25 arbitrary units above background, as previously described (15). The diameters of ≥ 200 muscle fibers per muscle were measured using the lesser diameter method, as recommended elsewhere (12).

Statistical analysis

We used paired *t*-tests to compare within-subject samples (Figs. 1, 2*D*-*F*, 3, 5*B*, 6*A*-*D*, 7, and 8), and unpaired *t*-tests for all other comparisons between two groups (Figs. 2*A*-*C* and *G*-*I*, 5*A* and *C*, and 6*E*-*G*). We used a one-way ANOVA with Dunnett's post hoc test to compare the three groups in Figs. 4*A* and 4*C*. In microarray analyses of limb immobilization and p21 overexpression, statistical significance was arbitrarily defined as $P \leq 0.05$. In microarray analysis of spermine overexpression, statistical significance was arbitrarily defined as $P \leq 0.01$. In gene set enrichment analysis (GSEA), statistical significance was defined as $P \leq 0.05$ and FDR ≤ 0.25, as previously described (34).

RESULTS

Conditions That Cause Skeletal Muscle Atrophy Strongly Repress Spermine Oxidase Expression in Skeletal Muscle

Our overall goal in this study was to identify a skeletal muscle protein whose function helps to maintain muscle mass, but is inhibited by conditions that cause muscle atrophy. We reasoned that such a protein: 1) might be reduced in atrophic skeletal muscle; 2) might begin to be reduced as muscle atrophy begins to occur; and 3) might be decreased via a reduction in the mRNA that encodes this protein.

To begin to test this hypothesis, we used unbiased, genome-wide mRNA expression arrays to search for mRNAs that are strongly repressed in the mouse tibialis anterior (TA) muscle by a short period of limb immobilization (three days). Importantly, three days of limb immobilization is sufficient to induce a small but significant amount of skeletal muscle atrophy (17). Our mRNA expression arrays were Illumina Mouse Ref-8 v2.0 BeadChip arrays, which contain 25,697 probes directed against 17,192 unique mRNAs, including five probes directed against *spermine oxidase* mRNA. Interestingly, three days of limb immobilization strongly repressed the signals from all five *spermine oxidase* probes, which represented the 1st, 2nd, 5th, 12th, and 15th most repressed annotated probe signals from immobilized TA muscle (Fig. 1*A*). We performed qPCR analysis to confirm that three days of limb immobilization significantly reduced the amount of *spermine oxidase* mRNA in TA muscle (Fig. 1*B*).

Spermine oxidase is an FAD-dependent oxidase that specifically catabolizes spermine into spermidine, 3-aminopropanal, and H_2O_2 (8, 9). Its role in the control of skeletal muscle mass was unknown. To determine if limb immobilization also reduced spermine oxidase protein, we performed immunoblot analysis. Under basal conditions, TA muscle contained a high level of spermine oxidase protein (Fig. 1*C*), and the molecular weight of this protein (65 kDa) was consistent with it being the longest (mu) isoform of spermine oxidase, which is catalytically active (9). As predicted by its effects on *spermine*

oxidase mRNA, three days of limb immobilization significantly reduced the level of spermine oxidase protein in TA muscle (Fig. 1*C*). Moreover, three days of limb immobilization significantly increased the level of spermine in TA muscle, consistent with reduced spermine oxidase activity (Fig. 1*D*). Interestingly, muscle immobilization did not alter the level of spermidine (the levels were 18.9 ± 2.3 mg spermidine/g mobile muscle and 18.5 ± 1.1 mg spermidine/g immobile muscle; $P = 0.96$), suggesting that other enzymes or transporters are able to maintain the level of spermidine when spermine oxidase activity is reduced.

The finding that muscle immobilization reduced spermine oxidase expression led us to investigate whether similar changes might also occur during other conditions that cause muscle atrophy, such as 24 hours of fasting (15), seven days of muscle denervation (14), and 22 months of aging (50). Like muscle immobilization, fasting reduced *spermine oxidase* mRNA and spermine oxidase protein in skeletal muscle (Fig. 2*A*-*B*), and it increased the level of spermine in skeletal muscle (Fig. 2*C*). Similarly, muscle denervation reduced *spermine oxidase* mRNA and spermine oxidase protein (Figs. 2*D*-*E*), and it increased the level of spermine in skeletal muscle (Fig. 2*F*). Furthermore, 22-month-old mice, which exhibit age-related muscle atrophy (50), contained reduced levels of *spermine oxidase* mRNA and spermine oxidase protein and an increased amount of spermine in their skeletal muscles relative to 6-month-old control mice (Figs. 2*G*-*I*). For reasons that are not clear to us at this point, the basal level of spermine varied somewhat from experiment to experiment (see Figs. 1*D*, 2*C*, 2*F*, and 2*I*). However, the relative level of spermine was consistently higher during conditions that reduced spermine oxidase expression and cause muscle atrophy (see Figs. 1*D*, 2*C*, 2*F*, and 2*I*). Thus, during muscle immobilization, fasting, muscle denervation, and aging, skeletal muscle atrophy is associated with a significant reduction in spermine oxidase and a relative increase in the level of spermine.

Spermine Oxidase Has a Positive Effect on Muscle Fiber Size that Protects Against Muscle Fiber Atrophy

Because spermine oxidase was reduced by conditions that cause muscle atrophy, we hypothesized that spermine oxidase might have a positive effect on skeletal muscle fiber size, which decreases during muscle atrophy. To test this hypothesis, we used *in vivo* electroporation (a method that transfects terminally differentiated skeletal muscle fibers, but not satellite cells or connective tissue cells (42)) to transfect mouse TA muscle fibers with a plasmid encoding spermine oxidase. In each mouse, the contralateral TA muscle was transfected with an empty plasmid and served as an intrasubject control. As expected, transfection of spermine oxidase plasmid increased *spermine oxidase* mRNA and spermine oxidase protein (Figs. 3*A*-*B*), and it reduced the level of spermine in skeletal muscle (Fig. 3*C*). Importantly, increased expression of spermine oxidase led to an increase in muscle fiber size (Figs. 3*D*-*E*).

As an additional control, we transfected skeletal muscle fibers with plasmid encoding spermine oxidase (H82E/T558Y), a spermine oxidase construct that contains two point mutations that abolish spermine oxidase activity (47). Although spermine oxidase (H82E/T558Y) was highly expressed (Figs. 3*F*-*G*), it did not decrease spermine levels (Fig. 3*H*) or increase muscle fiber size (Figs. 3*I*-*J*), suggesting that catalytic activity may be required for spermine oxidase's positive effect on muscle fiber size. Interestingly, spermine oxidase (H82E/T558Y) appeared to have dominant negative effect, as it increased spermine and decreased muscle fiber size (Figs. 3*H*-*J*).

The finding that spermine oxidase (H82E/T558Y) reduced muscle fiber size, coupled with the finding that spermine oxidase expression is reduced during muscle atrophy, suggested that reduced spermine oxidase activity might be sufficient to induce muscle fiber atrophy. To test this hypothesis, we used RNA interference to reduce the level of spermine oxidase in skeletal muscle fibers. To this end, we generated two artificial microRNA (miR) constructs (*miR-Spermine Oxidase #1* and *miR-Spermine Oxidase #2*) that

target distinct regions of the *spermine oxidase* mRNA and specifically reduce spermine oxidase protein (Fig. 4*A*). We then transfected skeletal muscle fibers *in vivo* with plasmids encoding either *miR-Spermine Oxidase #1*, *miR-Spermine Oxidase #2*, or a nontargeting control miRNA (*miR-Control*). We found that knockdown of spermine oxidase with either *miR-Spermine Oxidase* construct markedly reduced muscle fiber size (Figs. 4*B-C*). Taken together, these data indicate that reduced spermine oxidase expression (as seen during immobilization, fasting, denervation, and aging) is sufficient to induce muscle fiber atrophy.

To determine if forced expression of spermine oxidase might increase the size of atrophic muscle fibers, we transfected skeletal muscle fibers with plasmid encoding wild-type spermine oxidase, and then induced muscle atrophy via limb immobilization (Fig. 5*A*), fasting (Fig. 5*B*), or muscle denervation (Fig. 5C). In each of these atrophy conditions, forced expression of spermine oxidase increased muscle fiber size, suggesting that decreased spermine oxidase expression is both necessary and sufficient for muscle fiber atrophy.

p21 Mediates the Repression of Spermine Oxidase During Muscle Atrophy

Based on our findings that decreased spermine oxidase expression promotes muscle fiber atrophy, and that the reduction in spermine oxidase expression during muscle atrophy can be explained at least in part by a reduction in *spermine oxidase* mRNA, we investigated whether *spermine oxidase* mRNA might be reduced by a protein that is known to actively promote muscle atrophy, p21. In sharp contrast to spermine oxidase, p21 is expressed at low levels in healthy skeletal muscle, and it is highly induced by conditions that decrease spermine oxidase expression and induce muscle atrophy (i.e. aging, denervation, fasting, hindlimb unloading, amyotrophic lateral sclerosis (ALS), and critical illness) (1, 5, 15, 16, 20, 22, 26, 30, 44, 48, 49). Furthermore, increased p21 expression is sufficient to induce muscle fiber atrophy, and it is required for muscle atrophy induced by three days of muscle immobilization (17). These considerations led us to hypothesize that p21 might be responsible for repressing *spermine oxidase* mRNA during muscle atrophy.

To begin to test this hypothesis, we transfected skeletal muscle fibers with a plasmid encoding p21, which is sufficient to induce muscle fiber atrophy (17). We then used Illumina Mouse Ref-8 v2.0 BeadChip arrays to analyze the effect of p21 on skeletal muscle mRNA levels. Remarkably, p21 overexpression strongly repressed the signals from all five *spermine oxidase* probes, which represented the 1st, 2nd, 3rd, 4th, and 9th most repressed annotated probe signals from muscles overexpressing p21 (out of >25,000 measured probe signals) (Fig. 6*A*). qPCR analysis confirmed that p21 overexpression significantly reduced the level of *spermine oxidase* mRNA in skeletal muscle (Fig. 6*B*). Consistent with its effect on *spermine oxidase* mRNA, p21 also reduced the level of spermine oxidase protein (Fig. 6*C*) and increased the level of spermine in skeletal muscle (Fig. 6*D*). These data indicate that increased p21 expression is sufficient to reduce spermine oxidase expression and activity in skeletal muscle.

To determine whether p21 is required for the reduction of spermine oxidase expression during muscle atrophy, we transfected skeletal muscle fibers with plasmids encoding either *miR-Control* or *miR-p21*, an artificial microRNA that specifically reduces p21 expression in skeletal muscle and inhibits muscle fiber atrophy induced by limb immobilization (17). We then induced endogenous p21 expression by immobilizing the transfected skeletal muscles for three days. As expected, *miR-p21* decreased *p21* mRNA and p21 protein in immobilized muscle (Figs. 6*E-F*). Importantly, this reduction in p21 was accompanied by an increase in *spermine oxidase* mRNA and spermine oxidase protein (Figs. 6*E-F*) and a reduction in the level of spermine in skeletal muscle (Fig. 6*G*). Taken together, these data indicate that p21 is at least partially required for the repression of spermine oxidase during immobilization-induced muscle atrophy.

To test whether forced expression of spermine oxidase might reduce p21-mediated muscle fiber atrophy, we overexpressed p21 in the absence and presence of plasmid encoding spermine oxidase (Fig. 7*A*). We found that spermine oxidase significantly increased muscle fiber size in the presence of p21 (Figs. 7*B-D*).

348 Since p21 induces muscle fiber atrophy (17), these data suggest that the repression of spermine oxidase is
349 an important downstream event in p21-mediated muscle atrophy.
350
351 ***Spermine Oxidase Generates Changes in Skeletal Muscle mRNA Expression that Are Opposite to the***
352 ***Changes that Occur During Muscle Atrophy***
353 To begin to understand the mechanism by which spermine oxidase maintains muscle fiber size, we
354 considered the fact that spermine is a major cationic component of cells, capable of binding to acidic sites
355 on proteins and nucleic acids and influencing cellular gene expression (37). From this perspective, we
356 hypothesized that spermine oxidase might influence muscle fiber gene expression in a way that maintains
357 muscle fiber size and prevents muscle fiber atrophy. Furthermore, because spermine oxidase is reduced
358 during muscle atrophy (at least in part due to the actions of p21), we hypothesized that important effects
359 of spermine oxidase would be opposed by a bona fide atrophy stimulus (muscle immobilization) and by
360 p21 overexpression. To begin to test this hypothesis, we transfected skeletal muscle fibers with plasmid
361 encoding wild-type spermine oxidase, and then determined effects of spermine oxidase on skeletal muscle
362 mRNA levels with Illumina Mouse Ref-8 v2.0 BeadChip arrays. We then compared the effects of
363 spermine oxidase overexpression to the effects of muscle immobilization (Fig. 1*A*) and the effects of p21
364 overexpression (Fig. 6*A*).
365
366 To identify mRNA transcripts that might contribute to the positive effects of spermine oxidase on muscle
367 fiber size, we searched for skeletal muscle mRNAs that were: 1) increased by spermine oxidase, and
368 decreased by muscle immobilization and p21; or 2) decreased by spermine oxidase, and increased by
369 muscle immobilization and p21. Altogether, we identified 21 mRNAs (including *spermine oxidase* itself)
370 that were increased by spermine oxidase and decreased by immobilization and p21; and 14 mRNAs that
371 were decreased by spermine oxidase and increased by immobilization and p21 (Fig. 8*A*). Not
372 surprisingly, most of these mRNAs encode proteins that have not been studied in the context of skeletal
373 muscle atrophy. However, it was interesting that spermine oxidase increased (and immobilization and

p21 decreased) several mRNAs involved in mitochondrial structure and function (e.g. the mRNA encoding mitofusin-2, which is required for maintenance of skeletal muscle mass (10)) (Fig. 8*A*). It was also notable that spermine oxidase decreased (and immobilization and p21 increased) mRNAs encoding the myogenic regulatory factor myogenin (Fig. 8*A*), which promotes muscle atrophy (35). We used qPCR to confirm that *mitofusin-2* mRNA was decreased by immobilization and p21 and increased by spermine oxidase, and to confirm that *myogenin* mRNA was increased by immobilization and p21 and decreased by spermine oxidase (Fig. 8*B*). As predicted by these changes in mRNA levels, immunoblot analyses showed that spermine oxidase increased mitofusin-2 protein (Fig. 8*C*) and decreased myogenin protein (Fig. 8*D*).

To identify cellular processes that are induced or repressed by spermine oxidase and regulated in the opposite direction by immobilization and p21, we performed gene set enrichment analysis (34). By this method, we identified 10 gene sets that were induced by spermine oxidase and repressed by immobilization and p21 (Fig. 9); the majority of these gene sets represented cellular processes that contribute to mitochondrial biogenesis and function, which are known to be critical for the maintenance of muscle fiber size and muscle mass. Conversely, 21 gene sets were repressed by spermine oxidase and induced by immobilization and p21 (Fig. 9); many of these gene sets represented cellular processes that are known to be involved in muscle atrophy, including inflammation, altered protein metabolism, and extracellular matrix remodeling. Collectively, these data indicate that spermine oxidase influences skeletal muscle gene expression in a manner that helps to maintain muscle fiber size and prevent muscle fiber atrophy. These findings may also begin to explain how p21 and reduced expression of spermine oxidase trigger skeletal muscle atrophy.

DISCUSSION

In the current study, we sought to discover a previously unrecognized mechanism of muscle atrophy by identifying a skeletal muscle protein that helps to protect muscle mass, but is strongly and specifically reduced by conditions that cause muscle atrophy. To this end, we performed an unbiased search, which revealed spermine oxidase, a protein not previously known to play a role in muscle atrophy.

Our data indicate that spermine oxidase is expressed at a relatively high level in healthy skeletal muscle, where it contributes to a gene expression pattern that helps to maintain muscle fiber size and prevent muscle atrophy (Fig. 10). Our data also indicate that diverse atrophy stimuli (e.g. limb immobilization, fasting, muscle denervation, and aging) profoundly reduce *spermine oxidase* mRNA by upregulating skeletal muscle p21 expression. As a result, the level of spermine oxidase enzyme falls, and a new pattern of skeletal muscle gene expression emerges, leading to induction of pro-atrophy genes (e.g. *myogenin* and genes involved in inflammation and extracellular matrix remodeling) and repression of anti-atrophy genes (e.g. *mitofusin-2* and other genes involved in mitochondrial biogenesis and function). We speculate that this new pattern of skeletal muscle gene expression promotes atrophy of skeletal muscle fibers by impairing mitochondrial function, by stimulating inflammatory/stress signaling pathways, and perhaps by influencing other cellular processes that help to control muscle mass but have not yet been studied in the context of muscle atrophy.

In addition to identifying spermine oxidase as an important regulator of muscle gene expression and fiber size, the current study elucidates p21-mediated repression of spermine oxidase as a key mechanism of muscle atrophy. During muscle atrophy, p21 expression is upregulated by the transcription factors p53 and ATF4 (15, 17), and possibly other factors (Fig. 10). Increased expression of p21 is necessary and sufficient for muscle fiber atrophy (17), but the mechanism by which p21 causes muscle fiber atrophy was unknown. Our data indicate that p21 causes muscle atrophy at least in part by reducing *spermine*

oxidase mRNA. Further studies will be needed to determine whether p21 reduces *spermine oxidase* mRNA by decreasing its transcription or increasing its turnover, and whether p21 exerts these effects via a direct or indirect mechanism.

Understanding how spermine oxidase influences muscle gene expression is another important area for future investigation. Because spermine oxidase catalyzes the conversion of spermine to spermidine, H_2O_2 and 3-aminopropanal, we speculate that spermine oxidase may regulate muscle gene expression by directly altering the levels of one or more of these metabolites. In support of this idea, many studies have shown that polyamines such as spermine and spermidine can influence cellular gene expression in a variety of ways (reviewed in (37)). Our data indicate that a reduction in spermine oxidase expression (as occurs during muscle atrophy) is associated with a relative increase in the level of spermine, and not necessarily a change in the level of spermidine. It also seems possible that muscle gene expression might be sensitive to changes in the levels of H_2O_2 and/or 3-aminopropanal, which would be predicted to increase with spermine oxidase activity. H_2O_2 has been shown to influence gene expression (38), but the level of H_2O_2 in muscle is affected by many factors. We do not yet know the relative contribution of spermine oxidase activity to skeletal muscle H_2O_2. To our knowledge, potential effects of 3-aminopropanal on muscle gene expression have not been investigated. Further studies will be required to investigate these issues, and to test the alternative possibilities that: 1) spermine oxidase may regulate muscle gene expression by a mechanism that is independent of its known enzymatic activity, and 2) spermine oxidase may help to maintain muscle fiber size by mechanisms, direct or indirect, that are independent of changes in muscle gene expression.

Other outstanding issues are whether atrophy-associated changes in p21 and spermine oxidase expression occur in muscle fibers, satellite cells and/or other cell types residing in skeletal muscle, and whether these cell types are sensitive to changes in spermine oxidase activity. In addition, we do not yet know whether

447 spermine oxidase expression is restricted to specific fiber types, or if specific fiber types are more
448 responsive than others to spermine oxidase. These are all important areas for future investigation.
449
450 The current data indicate that reduced *spermine oxidase* expression may contribute to muscle atrophy
451 during a variety of stress conditions including immobilization, denervation, fasting and aging. Similarly,
452 skeletal muscle p21 expression increases in all of these conditions, suggesting that repression of *spermine*
453 *oxidase*, mediated by p21, may be a fundamentally conserved mechanism of skeletal muscle atrophy.
454 Additional work will be required to understand how the p21-spermine oxidase axis connects to other key
455 muscle atrophy pathways, such as those mediated by MuRF1, myostatin, FoxO, TWEAK, and Gadd45a
456 (5, 6, 14, 28, 36, 41). Interestingly, we found that forced expression of spermine oxidase stimulated
457 muscle fiber hypertrophy under basal conditions. Based on this finding, we speculate that spermine
458 oxidase may also contribute to skeletal muscle hypertrophy. In support of this idea, previous studies have
459 shown that at least some small molecules that reduce muscle atrophy and stimulate muscle hypertrophy
460 (androgens and ursolic acid) strongly upregulate *spermine oxidase* mRNA in skeletal muscle (24, 45).
461 Furthermore, the androgen receptor is required to maintain normal *spermine oxidase* expression in
462 skeletal muscle, as well as skeletal muscle mass (31). It is also interesting to note that changes in
463 polyamine levels have been associated with hypertrophy of cardiac myocytes (2, 3, 29, 43).
464
465 In summary, the current study identifies spermine oxidase as an important positive regulator of muscle
466 fiber size whose expression is strongly downregulated by conditions that cause muscle atrophy. This
467 reduction in spermine oxidase enables the atrophy process and represents a potential target for therapeutic
468 intervention.
469

REFERENCES

1. **Banduseela VC, Ochala J, Chen YW, Goransson H, Norman H, Radell P, Eriksson LI, Hoffman EP, and Larsson L**. Gene expression and muscle fiber function in a porcine ICU model. *Physiol Genomics* 39: 141-159, 2009.
2. **Bartolome J, Huguenard J, and Slotkin TA**. Role of ornithine decarboxylase in cardiac growth and hypertrophy. *Science* 210: 793-794, 1980.
3. **Bartolome JV, Trepanier PA, Chait EA, and Slotkin TA**. Role of polyamines in isoproterenol-induced cardiac hypertrophy: effects of alpha-difluoromethylornithine, an irreversible inhibitor of ornithine decarboxylase. *J Mol Cell Cardiol* 14: 461-466, 1982.
4. **Bodine SC**. Disuse-induced muscle wasting. *Int J Biochem Cell Biol* 45: 2200-2208, 2013.
5. **Bodine SC, Latres E, Baumhueter S, Lai VK, Nunez L, Clarke BA, Poueymirou WT, Panaro FJ, Na E, Dharmarajan K, Pan ZQ, Valenzuela DM, DeChiara TM, Stitt TN, Yancopoulos GD, and Glass DJ**. Identification of ubiquitin ligases required for skeletal muscle atrophy. *Science* 294: 1704-1708, 2001.
6. **Bongers KS, Fox DK, Ebert SM, Kunkel SD, Dyle MC, Bullard SA, Dierdorff JM, and Adams CM**. Skeletal muscle denervation causes skeletal muscle atrophy through a pathway that involves both Gadd45a and HDAC4. *Am J Physiol Endocrinol Metab* 305: E907-915, 2013.
7. **Caron AZ, Drouin G, Desrosiers J, Trensz F, and Grenier G**. A novel hindlimb immobilization procedure for studying skeletal muscle atrophy and recovery in mouse. *J Appl Physiol* 106: 2049-2059, 2009.
8. **Casero RA, and Pegg AE**. Polyamine catabolism and disease. *Biochem J* 421: 323-338, 2009.
9. **Cervelli M, Bellini A, Bianchi M, Marcocci L, Nocera S, Polticelli F, Federico R, Amendola R, and Mariottini P**. Mouse spermine oxidase gene splice variants. Nuclear subcellular localization of a novel active isoform. *Eur J Biochem* 271: 760-770, 2004.

10. **Chen H, Vermulst M, Wang YE, Chomyn A, Prolla TA, McCaffery JM, and Chan DC**. Mitochondrial fusion is required for mtDNA stability in skeletal muscle and tolerance of mtDNA mutations. *Cell* 141: 280-289, 2010.
11. **Dodd SL, Hain B, Senf SM, and Judge AR**. Hsp27 inhibits IKKbeta-induced NF-kappaB activity and skeletal muscle atrophy. *FASEB J* 23: 3415-3423, 2009.
12. **Dubowitz V, and Sewry CA**. *Muscle Biopsy: A Practical Approach*. Philadelphia: Saunders/Elsevier, 2007.
13. **Dyle MC, Ebert SM, Cook DP, Kunkel SD, Fox DK, Bongers KS, Bullard SA, Dierdorff JM, and Adams CM**. Systems-based discovery of tomatidine as a natural small molecule inhibitor of skeletal muscle atrophy. *J Biol Chem* 289: 14913-14924, 2014.
14. **Ebert SM, Dyle MC, Kunkel SD, Bullard SA, Bongers KS, Fox DK, Dierdorff JM, Foster ED, and Adams CM**. Stress-induced skeletal muscle Gadd45a expression reprograms myonuclei and causes muscle atrophy. *J Biol Chem* 287: 27290-27301, 2012.
15. **Ebert SM, Monteys AM, Fox DK, Bongers KS, Shields BE, Malmberg SE, Davidson BL, Suneja M, and Adams CM**. The transcription factor ATF4 promotes skeletal myofiber atrophy during fasting. *Mol Endocrinol* 24: 790-799, 2010.
16. **Edwards MG, Anderson RM, Yuan M, Kendziorski CM, Weindruch R, and Prolla TA**. Gene expression profiling of aging reveals activation of a p53-mediated transcriptional program. *BMC Genomics* 8: 80, 2007.
17. **Fox DK, Ebert SM, Bongers KS, Dyle MC, Bullard SA, Dierdorff JM, Kunkel SD, and Adams CM**. p53 and ATF4 mediate distinct and additive pathways to skeletal muscle atrophy during limb immobilization. *Am J Physiol Endocrinol Metab* 307: E245-261, 2014.
18. **Fry CS, and Rasmussen BB**. Skeletal muscle protein balance and metabolism in the elderly. *Curr Aging Sci* 4: 260-268, 2011.

19. **Giresi PG, Stevenson EJ, Theilhaber J, Koncarevic A, Parkington J, Fielding RA, and Kandarian SC**. Identification of a molecular signature of sarcopenia. *Physiol Genomics* 21: 253-263, 2005.

20. **Gonzalez de Aguilar JL, Niederhauser-Wiederkehr C, Halter B, De Tapia M, Di Scala F, Demougin P, Dupuis L, Primig M, Meininger V, and Loeffler JP**. Gene profiling of skeletal muscle in an amyotrophic lateral sclerosis mouse model. *Physiol Genomics* 32: 207-218, 2008.

21. **Hishiya A, Iemura S, Natsume T, Takayama S, Ikeda K, and Watanabe K**. A novel ubiquitin-binding protein ZNF216 functioning in muscle atrophy. *EMBO J* 25: 554-564, 2006.

22. **Ibebunjo C, Chick JM, Kendall T, Eash JK, Li C, Zhang Y, Vickers C, Wu Z, Clarke BA, Shi J, Cruz J, Fournier B, Brachat S, Gutzwiller S, Ma Q, Markovits J, Broome M, Steinkrauss M, Skuba E, Galarneau JR, Gygi SP, and Glass DJ**. Genomic and proteomic profiling reveals reduced mitochondrial function and disruption of the neuromuscular junction driving rat sarcopenia. *Mol Cell Biol* 33: 194-212, 2013.

23. **Kelleher AR, Kimball SR, Dennis MD, Schilder RJ, and Jefferson LS**. The mTORC1 signaling repressors REDD1/2 are rapidly induced and activation of p70S6K1 by leucine is defective in skeletal muscle of an immobilized rat hindlimb. *Am J Physiol Endocrinol Metab* 304: E229-236, 2013.

24. **Kunkel SD, Suneja M, Ebert SM, Bongers KS, Fox DK, Malmberg SE, Alipour F, Shields RK, and Adams CM**. mRNA expression signatures of human skeletal muscle atrophy identify a natural compound that increases muscle mass. *Cell Metab* 13: 627-638, 2011.

25. **Larsson L**. Experimental animal models of muscle wasting in intensive care unit patients. *Crit Care Med* 35: S484-487, 2007.

26. **Laure L, Suel L, Roudaut C, Bourg N, Ouali A, Bartoli M, Richard I, and Daniele N**. Cardiac ankyrin repeat protein is a marker of skeletal muscle pathological remodelling. *FEBS J* 276: 669-684, 2009.

27. **Lee D, and Goldberg AL**. SIRT1 protein, by blocking the activities of transcription factors FoxO1 and FoxO3, inhibits muscle atrophy and promotes muscle growth. *J Biol Chem* 288: 30515-30526, 2013.

28. **Lee SJ**. Regulation of muscle mass by myostatin. *Annu Rev Cell Dev Biol* 20: 61-86, 2004.

29. **Lin Y, Zhang X, Wang L, Zhao Y, Li H, Xiao W, Xu C, and Liu J**. Polyamine depletion attenuates isoproterenol-induced hypertrophy and endoplasmic reticulum stress in cardiomyocytes. *Cell Physiol Biochem* 34: 1455-1465, 2014.

30. **Llano-Diez M, Gustafson AM, Olsson C, Goransson H, and Larsson L**. Muscle wasting and the temporal gene expression pattern in a novel rat intensive care unit model. *BMC Genomics* 12: 602, 2011.

31. **MacLean HE, Chiu WS, Notini AJ, Axell AM, Davey RA, McManus JF, Ma C, Plant DR, Lynch GS, and Zajac JD**. Impaired skeletal muscle development and function in male, but not female, genomic androgen receptor knockout mice. *FASEB J* 22: 2676-2689, 2008.

32. **Mammucari C, Milan G, Romanello V, Masiero E, Rudolf R, Del Piccolo P, Burden SJ, Di Lisi R, Sandri C, Zhao J, Goldberg AL, Schiaffino S, and Sandri M**. FoxO3 controls autophagy in skeletal muscle in vivo. *Cell Metab* 6: 458-471, 2007.

33. **Mittal A, Bhatnagar S, Kumar A, Lach-Trifilieff E, Wauters S, Li H, Makonchuk DY, Glass DJ, and Kumar A**. The TWEAK-Fn14 system is a critical regulator of denervation-induced skeletal muscle atrophy in mice. *J Cell Biol* 188: 833-849, 2010.

34. **Mootha VK, Lindgren CM, Eriksson KF, Subramanian A, Sihag S, Lehar J, Puigserver P, Carlsson E, Ridderstrale M, Laurila E, Houstis N, Daly MJ, Patterson N, Mesirov JP, Golub TR, Tamayo P, Spiegelman B, Lander ES, Hirschhorn JN, Altshuler D, and Groop LC**. PGC-1alpha-responsive genes involved in oxidative phosphorylation are coordinately downregulated in human diabetes. *Nat Genet* 34: 267-273, 2003.

35. **Moresi V, Williams AH, Meadows E, Flynn JM, Potthoff MJ, McAnally J, Shelton JM, Backs J, Klein WH, Richardson JA, Bassel-Duby R, and Olson EN**. Myogenin and class II HDACs control neurogenic muscle atrophy by inducing E3 ubiquitin ligases. *Cell* 143: 35-45, 2010.

36. **Paul PK, Bhatnagar S, Mishra V, Srivastava S, Darnay BG, Choi Y, and Kumar A**. The E3 ubiquitin ligase TRAF6 intercedes in starvation-induced skeletal muscle atrophy through multiple mechanisms. *Mol Cell Biol* 32: 1248-1259, 2012.

37. **Pegg AE**. Mammalian polyamine metabolism and function. *IUBMB Life* 61: 880-894, 2009.

38. **Powers SK, Duarte J, Kavazis AN, and Talbert EE**. Reactive oxygen species are signalling molecules for skeletal muscle adaptation. *Exp Physiol* 95: 1-9, 2010.

39. **Sacheck JM, Hyatt JP, Raffaello A, Jagoe RT, Roy RR, Edgerton VR, Lecker SH, and Goldberg AL**. Rapid disuse and denervation atrophy involve transcriptional changes similar to those of muscle wasting during systemic diseases. *FASEB J* 21: 140-155, 2007.

40. **Sandri M, Lin J, Handschin C, Yang W, Arany ZP, Lecker SH, Goldberg AL, and Spiegelman BM**. PGC-1alpha protects skeletal muscle from atrophy by suppressing FoxO3 action and atrophy-specific gene transcription. *Proc Natl Acad Sci U S A* 103: 16260-16265, 2006.

41. **Sandri M, Sandri C, Gilbert A, Skurk C, Calabria E, Picard A, Walsh K, Schiaffino S, Lecker SH, and Goldberg AL**. Foxo transcription factors induce the atrophy-related ubiquitin ligase atrogin-1 and cause skeletal muscle atrophy. *Cell* 117: 399-412, 2004.

42. **Sartori R, Milan G, Patron M, Mammucari C, Blaauw B, Abraham R, and Sandri M**. Smad2 and 3 transcription factors control muscle mass in adulthood. *Am J Physiol Cell Physiol* 296: C1248-1257, 2009.

43. **Shantz LM, Feith DJ, and Pegg AE**. Targeted overexpression of ornithine decarboxylase enhances beta-adrenergic agonist-induced cardiac hypertrophy. *Biochem J* 358: 25-32, 2001.

44. **Stevenson EJ, Giresi PG, Koncarevic A, and Kandarian SC**. Global analysis of gene expression patterns during disuse atrophy in rat skeletal muscle. *J Physiol* 551: 33-48, 2003.

45. **Svensson J, Moverare-Skrtic S, Windahl S, Swanson C, and Sjogren K**. Stimulation of both estrogen and androgen receptors maintains skeletal muscle mass in gonadectomized male mice but mainly via different pathways. *J Mol Endocrinol* 45: 45-57, 2010.

46. **Tan BH, and Fearon KC**. Cachexia: prevalence and impact in medicine. *Curr Opin Clin Nutr Metab Care* 11: 400-407, 2008.

47. **Tavladoraki P, Cervelli M, Antonangeli F, Minervini G, Stano P, Federico R, Mariottini P, and Polticelli F**. Probing mammalian spermine oxidase enzyme-substrate complex through molecular modeling, site-directed mutagenesis and biochemical characterization. *Amino Acids* 40: 1115-1126, 2011.

48. **Welle S, Brooks AI, Delehanty JM, Needler N, Bhatt K, Shah B, and Thornton CA**. Skeletal muscle gene expression profiles in 20-29 year old and 65-71 year old women. *Exp Gerontol* 39: 369-377, 2004.

49. **Welle S, Brooks AI, Delehanty JM, Needler N, and Thornton CA**. Gene expression profile of aging in human muscle. *Physiol Genomics* 14: 149-159, 2003.

50. **Wenz T, Rossi SG, Rotundo RL, Spiegelman BM, and Moraes CT**. Increased muscle PGC-1alpha expression protects from sarcopenia and metabolic disease during aging. *Proc Natl Acad Sci U S A* 106: 20405-20410, 2009.

FOOTNOTES

We thank Drs. Peter Snyder, Vitor Lira, Peter Rubenstein, and Daryl Granner for critical review of the manuscript, and Hannah McMahon for excellent technical assistance. This publication was made possible by funding from the National Institutes of Health (grants AR059115-04, F30AG04496401, F30AG04330401, 1F31AG04603801, and 5T32GM007337), the Department of Veterans Affairs Biomedical Laboratory Research & Development Service (grant IBX000976A), and the Fraternal Order of Eagles Diabetes Research Center at the University of Iowa. C.M.A. and S.M.E. hold equity in Emmyon, Inc. C.M.A. is a co-founder and officer of Emmyon, Inc.

620 **FIGURE LEGENDS**

621

622 **Figure 1. Limb immobilization decreases spermine oxidase in skeletal muscle.**

623 ***A:*** To identify skeletal muscle mRNAs that are most reduced by limb immobilization, we examined data
624 from a previous study (17). In that study, two month old C57BL/6 mice were subjected to unilateral
625 hindlimb immobilization for three days, and then mRNA from bilateral tibialis anterior (TA) muscles
626 (mobile and immobile) was analyzed with Illumina MouseRef-8 version 2.0 BeadChip arrays (n = 4
627 arrays per condition). In each mouse, probe signals from the immobilized TA were normalized to probe
628 signals from the contralateral (mobile) TA, and *P*-values were determined with paired *t*-tests. Statistical
629 significance was arbitrarily defined as $P \leq 0.05$. The figure shows the 15 annotated probe signals that
630 were most reduced by immobilization. ***B-D:*** Two month old C57BL/6 mice were subjected to unilateral
631 hindlimb immobilization for three days, and then bilateral TA muscles were harvested for analysis. ***B:***
632 qPCR analysis of *spermine oxidase* mRNA. n = 6 muscles per condition. ***C:*** Immunoblot analysis of
633 spermine oxidase. *Left,* representative immunoblot. *Right,* quantification; n = 4 muscles per condition.
634 Membranes were stained with Ponceau S to confirm equal loading. ***D:*** Quantification of spermine by
635 HPLC-MS. n = 8 muscles per condition. ***B-D:*** Data are means ± SEM; $*P \leq 0.05$.

636

637 **Figure 2. Fasting, muscle denervation, and aging decrease spermine oxidase in skeletal muscle.**

638 ***A-C:*** Two month old mice were fasted for 24 hours or allowed *ad libitum* access to food, and then TA
639 muscles from both conditions were harvested for analyses. ***A:*** qPCR analysis of *spermine oxidase*
640 mRNA. n = 8 muscles per condition. ***B:*** Immunoblot analysis of spermine oxidase. *Left,* representative
641 immunoblot. *Right,* quantification. n = 4 muscles per condition. ***C:*** Quantification of spermine by
642 HPLC-MS. n = 4 muscles per condition. ***D-F:*** Two month old mice were subjected to unilateral
643 hindlimb denervation for seven days, and then bilateral TA muscles were harvested for analyses. ***D:***
644 qPCR analysis of *spermine oxidase* mRNA. n = 4 muscles per condition. ***E:*** Immunoblot analysis of
645 spermine oxidase. *Left,* representative immunoblot. *Right,* quantification. n = 4 muscles per condition.

F: Quantification of spermine by HPLC-MS. n = 6 muscles per condition. ***G-I:*** TA and quadriceps muscles of six month old mice (control) and 22 month old mice (aged) were harvested under basal conditions. ***G:*** qPCR analysis of *spermine oxidase* mRNA in the TA. n = 4 muscles per condition. ***H:*** Immunoblot analysis of spermine oxidase in the quadriceps. *Left,* representative immunoblot. *Right,* quantification. n = 4 muscles per condition. ***I:*** HPLC-MS quantification of spermine in the quadriceps. n = 8-10 muscles per condition. ***A-I:*** Data are means ± SEM; **P* ≤ 0.05.

Figure 3. Spermine oxidase increases muscle fiber size.

A-E: In two month old mice, one TA was transfected with 20 μg *p-Spermine Oxidase* plus 2 μg *p-eGFP*, and the contralateral TA ("Control") was transfected with 20 μg empty plasmid (*pcDNA3*) plus 2 μg *p-eGFP*. eGFP served as a transfection marker and does not alter muscle fiber size. Bilateral TAs were harvested seven days post-transfection (*A-C*) or ten days post-transfection (*D-E*). ***A:*** qPCR analysis of *spermine oxidase* mRNA. n = 6 muscles per condition. ***B:*** Immunoblot analysis of spermine oxidase protein. ***C:*** Quantification of spermine by HPLC-MS. n = 12 muscles per condition. ***D-E:*** Histological analysis. ***D:*** Representative fluorescence microscopy images of skeletal muscle cross sections. ***E:*** *Left*, mean fiber diameter ± SEM from 7 muscles per condition. Values were 34.5 ± 0.5 μm in muscles transfected with *pcDNA3* and 39.5 ± 1.0 μm in muscles transfected with *p-Spermine Oxidase*; **P* ≤ 0.001. *Right*, fiber size distributions. ***F-J:*** In two month old mice, one TA was transfected with 20 μg *p-Spermine Oxidase(H82E/T558Y)* plus 2 μg *p-eGFP*, and the contralateral TA ("Control") was transfected with 20 μg *pcDNA3* plus 2 μg *p-eGFP*. Bilateral TAs were harvested seven days post-transfection (*F-H*) or ten days post-transfection (*I-J*). ***F:*** qPCR analysis of *spermine oxidase* mRNA. n = 8 muscles per treatment. ***G:*** Immunoblot analysis of spermine oxidase protein. ***H:*** Quantification of spermine by HPLC-MS. n = 6 muscles per condition. ***I-J:*** Histological analysis. ***I:*** Representative images. ***J:*** *Left*, mean fiber diameter from 6 muscles per condition. Values were 37.9 ± 0.7 μm in muscles transfected

with *pcDNA3* and 34.8 ± 0.4 μm in muscles transfected with *p-Spermine Oxidase(H82E/T558Y)*; **P* ≤ 0.01. *Right*, fiber size distributions. ***A-C*** and ***F-H:*** Data are means ± SEM; **P* ≤ 0.05.

Figure 4. Decreased spermine oxidase expression is sufficient to induce skeletal muscle fiber atrophy.

A-C: TA muscles in two month old mice were transfected with either 20 μg *p-miR-Control*, 20 μg *p-miR-Spermine Oxidase #1,* or 20 μg *p-miR-Spermine Oxidase #2*, and then analyzed ten days post-transfection. ***A:*** Immunoblot analysis of spermine oxidase. *Top,* representative immunoblots. *Bottom,* quantification. Data are means ± SEM; n = 4 muscles per condition; **P* ≤ 0.05. ***B-C:*** Histological analysis. ***B:*** Representative fluorescence microscopy images of skeletal muscle cross sections. ***C:*** *Left*, mean fiber diameter ± SEM from 4 muscles per condition. Values were 40.6 ± 0.3 μm in muscles transfected with *miR-Control*, 32.6 ± 0.2 μm in muscles transfected with *p-miR-Spermine Oxidase #1*, and 33.3 ± 0.3 μm in muscles transfected with *p-miR-Spermine Oxidase #2*; **P* ≤ 0.01 one way ANOVA with Dunnett's post test. *Right*, fiber size distributions.

Figure 5. Forced expression of spermine oxidase increases muscle fiber size in multiple models of muscle atrophy.

A-C: TA muscles in two month old mice were transfected with either 20 μg empty plasmid (*pcDNA3*) plus 2 μg *p-eGFP* or 20 μg *p-Spermine Oxidase* plus 2 μg *p-eGFP*, and then subjected to atrophy stimuli one week later, as described below. ***A:*** Transfected TA muscles were immobilized for ten days before histological analysis. *Left,* representative fluorescence microscopy images of skeletal muscle cross sections. *Middle*, mean fiber diameter ± SEM from 6 muscles per condition. Values were 33.00 ± 0.92 μm in muscles transfected with *pcDNA3*, and 36.34 ± 0.30 μm in muscles transfected with *p-Spermine Oxidase*; **P* ≤ 0.01. *Right,* fiber size distributions. ***B:*** Mice were fasted for 24 hours, and then transfected TA muscles were used for histological analysis. *Left,* representative images. *Middle*, mean fiber diameter

± SEM from 4 muscles per condition. Values were 34.7 ± 0.6 μm in muscles transfected with *pcDNA3*, and 38.0 ± 0.4 μm in muscles transfected with *p-Spermine Oxidase*; **P* ≤ 0.01. *Right,* fiber size distributions. ***C:*** Transfected TA muscles were denervated for ten days before histological analysis. *Left,* representative images. *Middle*, mean fiber diameter ± SEM from 5-6 muscles per condition. Values were 26.9 ± 0.3 μm in muscles transfected with *pcDNA3*, and 30.6 ± 0.4 μm in muscles transfected with *p-Spermine Oxidase*; **P* ≤ 0.001. *Right,* fiber size distributions.

Figure 6. p21, a mediator of skeletal muscle atrophy, reduces spermine oxidase expression in skeletal muscle.

A-D: In two month old mice, one TA muscle was transfected with 20 μg *p-p21*, and the contralateral TA was transfected with 20 μg empty plasmid (*pcDNA3*). Transfected muscles were harvested for analyses seven days post-transfection. ***A:*** mRNA was analyzed with Illumina Mouse Ref-8 v2.0 BeadChip arrays (n = 4 arrays per condition). In each mouse, probe signals from the TA overexpressing p21 were normalized to probe signals from the contralateral, control-transfected TA. *P*-values were determined with paired *t*-tests, and statistical significance was arbitrarily defined as $P \leq 0.05$. The figure shows the 10 annotated probe signals that were most reduced by p21 overexpression. ***B:*** qPCR analysis of *p21* and *spermine oxidase* mRNAs. n = 6 muscles per condition. ***C:*** Immunoblot analysis of p21 and spermine oxidase. *Left,* representative immunoblots. *Right,* quantification of spermine oxidase. n = 4 muscles per condition. ***D:*** Quantification of spermine by HPLC-MS. n = 6 muscles per condition**.** ***E-G:*** TA muscles in two month old mice were transfected with 20 μg *p-miR-p21* or 20 μg *p-miR-Control*. One week later, transfected TA muscles were immobilized for three days and then harvested for analysis. ***E:*** qPCR analysis of *p21* and *spermine oxidase* mRNAs. n = 6 muscles per condition. ***F:*** Immunoblot analysis of p21 and spermine oxidase. *Left,* representative immunoblots. *Right,* quantification of spermine oxidase. n = 4 muscles per condition. ***G:*** Quantification of spermine by HPLC-MS. n = 8 muscles per condition. ***B-G:*** Data are means ± SEM; **P* ≤ 0.05.

Figure 7. Forced expression of spermine oxidase increases muscle fiber size in the presence of p21. ***A-C:*** In two month old mice, one TA muscle was co-transfected with 10 μg of *p-p21*, 20 μg *p-Spermine Oxidase,* and 2 μg *p-eGFP*. The contralateral TA was co-transfected with 10 μg *p-p21,* 20 μg *pcDNA3*, and 2 μg *p-eGFP*. ***A:*** Muscles were harvested seven days post-transfection for immunoblot analysis of p21 and spermine oxidase. ***B-D:*** Muscles were harvested ten days post-transfection for histologic analysis. ***B:*** Representative fluorescence microscopy images of skeletal muscle cross sections. ***C:*** Mean fiber diameter ± SEM from 6 muscles per condition. Values were 30.7 ± 0.5 μm in muscles transfected with *pcDNA3*, and 35.3 ± 0.5 μm in muscles transfected with *p-Spermine Oxidase*; $*P \leq 0.001$. ***D:*** Fiber size distributions.

Figure 8. Skeletal muscle mRNAs that are significantly induced or repressed by spermine oxidase overexpression, and regulated in the opposite direction by muscle immobilization and p21 overexpression.

A: To determine effects of spermine oxidase on muscle mRNA levels in two month old mice, one TA muscle was transfected with 20 μg *p-Spermine Oxidase*, and the contralateral TA was transfected with 20 μg empty plasmid (*pcDNA3*). mRNA from transfected muscles was harvested seven days post-transfection and analyzed with Illumina Mouse Ref-8 v2.0 BeadChip arrays (n = 4 arrays per condition). In each mouse, probe signals from the TA overexpressing spermine oxidase were normalized to probe signals from the contralateral, control-transfected TA, and *P*-values were determined with paired *t*-tests. Statistical significance was arbitrarily defined as $P \leq 0.01$. We then used these data in conjunction with data from the experiments described in Figures 1*A* and 6*A* to identify skeletal muscle mRNAs that were: 1) increased by spermine oxidase overexpression, and decreased by immobilization and p21 overexpression; or 2) decreased by spermine oxidase overexpression, and increased by immobilization and p21 overexpression. Those mRNAs are shown in the figure. ***B:*** qPCR analysis of *spermine oxidase*

(*Smox*), *mitofusin-2* (*Mfn2*), *p21*, and *myogenin* (*Myog*) mRNAs under the same conditions as in *A*. n = 5-6 TAs per condition. * $P \leq 0.05$. N.S.: $P > 0.05$. ***C-D:*** In two month old mice, one TA muscle was transfected with 20 μg *p-Spermine Oxidase*, and the contralateral TA was transfected with 20 μg empty plasmid (*pcDNA3*). Bilateral TA muscles were harvested seven days post-transfection and used for immunoblot analyses of mitofusin-2 (***C***) or myogenin (***D***). *Left,* representative immunoblots. *Right,* quantification; n = 4 muscles per condition. Membranes were stained with Ponceau S to confirm equal loading. Data are means ± SEM; *$P \leq 0.05$.

Figure 9. KEGG and Reactome gene sets that are significantly induced or repressed by spermine oxidase overexpression, and regulated in the opposite direction by muscle immobilization and p21 overexpression.

We performed gene set enrichment analysis of data described in Figures 1A, 6A, and 8A to identify KEGG and Reactome gene sets that were significantly: 1) induced (enriched) by spermine oxidase overexpression, and repressed (depleted) by immobilization and p21 overexpression; or 2) repressed by spermine oxidase overexpression, and induced by immobilization and p21 overexpression. Statistical significance was defined as $P \leq 0.05$ and FDR ≤ 0.25, as previously described (34).

Figure 10. Proposed relationship between muscle atrophy stimuli, p21 expression, spermine oxidase expression, skeletal muscle gene expression, and skeletal muscle atrophy.

Figure 1

A **Skeletal Muscle mRNAs Most Reduced by 3 Days of Limb Immobilization**

Probe Rank	Log_2 Change	mRNA	Encoded Protein
1	**-2.26**	***Smox***	**Spermine Oxidase**
2	**-2.25**	***Smox***	**Spermine Oxidase**
3	-2.25	*Kcnc1*	Potassium Voltage-gated Channel, Shaw-related Subfamily, Member 1
4	-2.09	*Mettl21c*	Methyltransferase-like 21C
5	**-1.99**	***Smox***	**Spermine Oxidase**
6	-1.88	*Tfrc*	Transferrin Receptor
7	-1.77	*Tfrc*	Transferrin Receptor
8	-1.75	*Mlf1*	Myeloid Leukemia Factor 1
9	-1.71	*Myl2*	Myosin, Light Polypeptide 2, Regulatory, Cardiac, Slow
10	-1.67	*Mlf1*	Myeloid Leukemia Factor 1
11	-1.62	*Kcna7*	Potassium Voltage-gated Channel, Shaker-related Subfamily, Member 7
12	**-1.60**	***Smox***	**Spermine Oxidase**
13	-1.58	*Gdap1*	Ganglioside-induced Differentiation-associated Protein 1
14	-1.54	*Map2k6*	Mitogen-activated Protein Kinase Kinase 6
15	**-1.51**	***Smox***	**Spermine Oxidase**

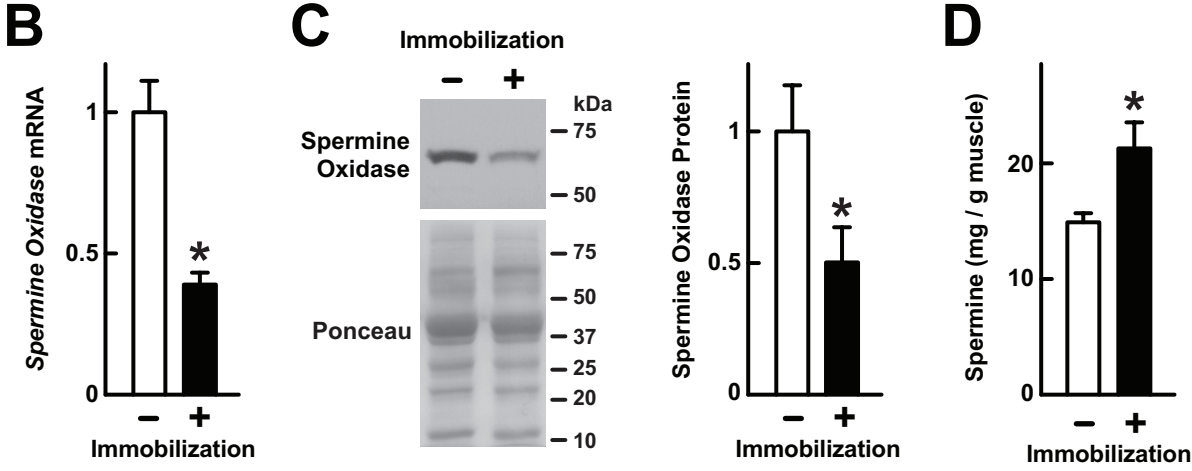

Figure 2

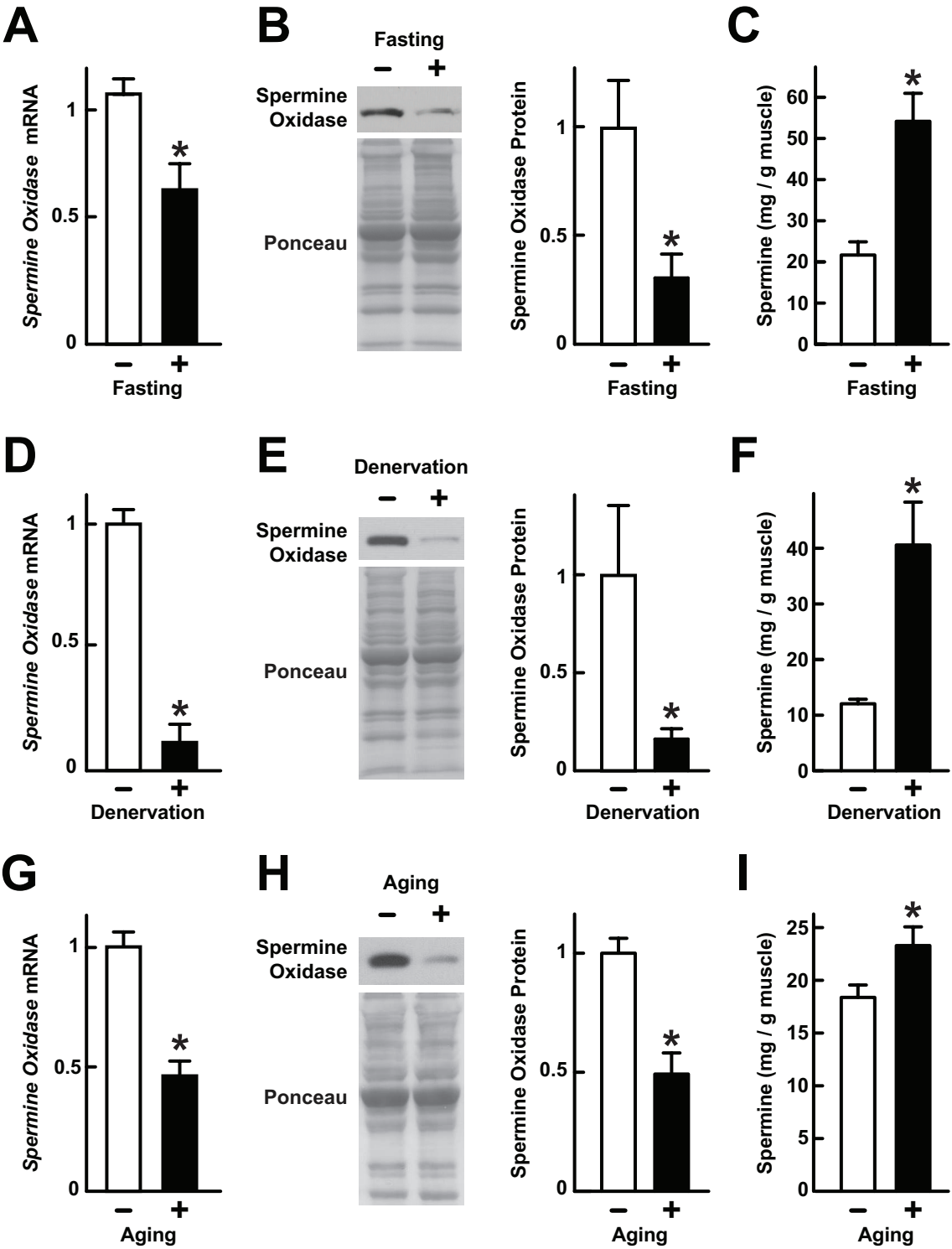
A
Spermine Oxidase mRNA
1
0.5
0
*
− +
Fasting
B
Fasting
− +
Spermine Oxidase
Ponceau
Spermine Oxidase Protein
1
0.5
0
*
− +
Fasting
C
Spermine (mg / g muscle)
60
50
40
30
20
10
0
*
− +
Fasting
D
Spermine Oxidase mRNA
1
0.5
0
*
− +
Denervation
E
Denervation
− +
Spermine Oxidase
Ponceau
Spermine Oxidase Protein
1
0.5
0
*
− +
Denervation
F
Spermine (mg / g muscle)
40
30
20
10
0
*
− +
Denervation
G
Spermine Oxidase mRNA
1
0.5
0
*
− +
Aging
H
Aging
− +
Spermine Oxidase
Ponceau
Spermine Oxidase Protein
1
0.5
0
*
− +
Aging
I
Spermine (mg / g muscle)
25
20
15
10
5
0
*
− +
Aging

Figure 3

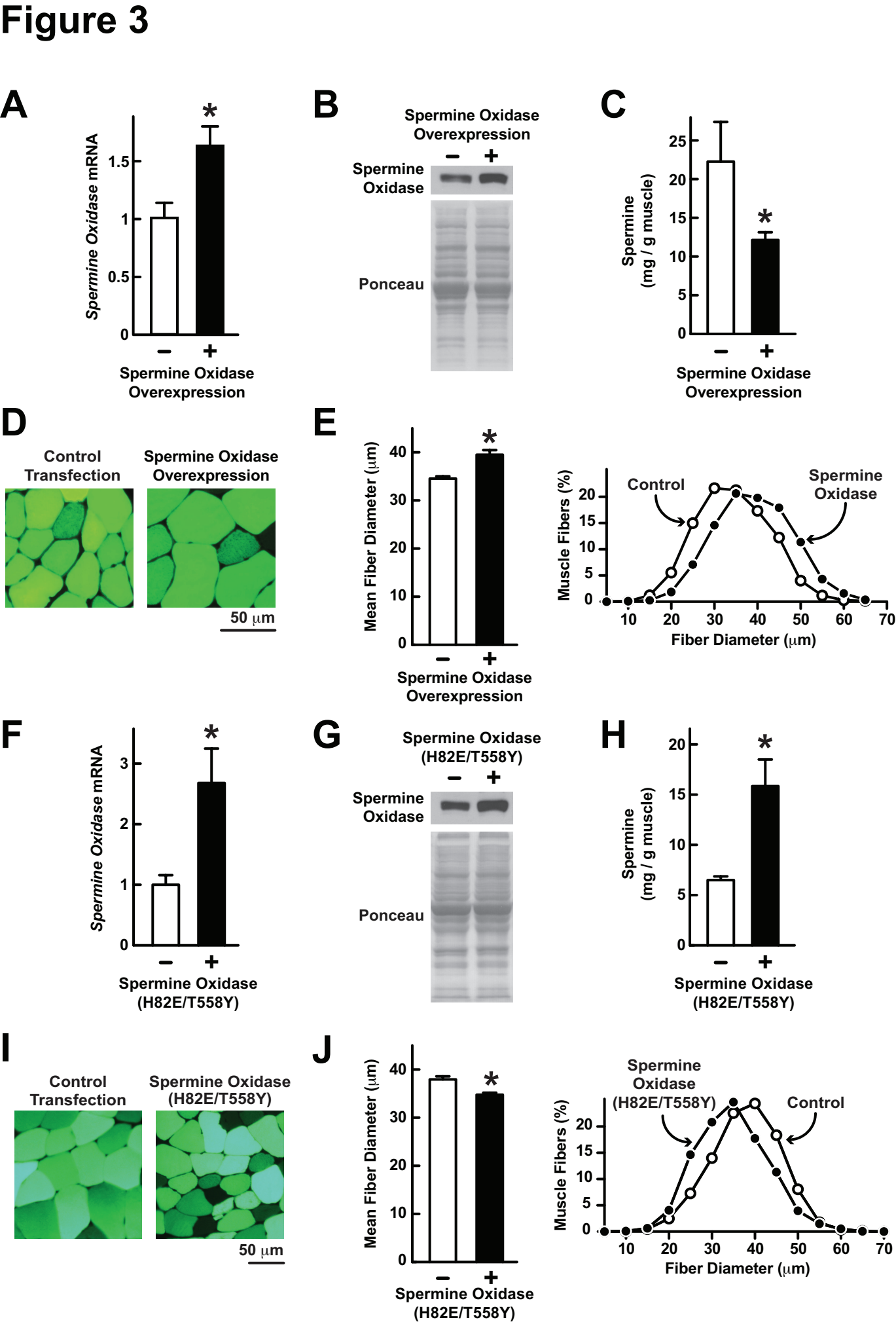
A
Spermine Oxidase mRNA
1.5
1
0.5
0
*
−
+
Spermine Oxidase Overexpression
B
Spermine Oxidase Overexpression
−
+
Spermine Oxidase
Ponceau
C
Spermine (mg / g muscle)
25
20
15
10
5
0
*
−
+
Spermine Oxidase Overexpression
D
Control Transfection
Spermine Oxidase Overexpression
50 μm
E
Mean Fiber Diameter (μm)
40
30
20
10
0
*
−
+
Spermine Oxidase Overexpression
Muscle Fibers (%)
Control
Spermine Oxidase
20
15
10
5
0
10
20
30
40
50
60
70
Fiber Diameter (μm)
F
Spermine Oxidase mRNA
3
2
1
0
*
−
+
Spermine Oxidase (H82E/T558Y)
G
Spermine Oxidase (H82E/T558Y)
−
+
Spermine Oxidase
Ponceau
H
Spermine (mg / g muscle)
20
15
10
5
0
*
−
+
Spermine Oxidase (H82E/T558Y)
I
Control Transfection
Spermine Oxidase (H82E/T558Y)
50 μm
J
Mean Fiber Diameter (μm)
40
30
20
10
0
*
−
+
Spermine Oxidase (H82E/T558Y)
Muscle Fibers (%)
Spermine Oxidase (H82E/T558Y)
Control
20
15
10
5
0
10
20
30
40
50
60
70
Fiber Diameter (μm)

Figure 4

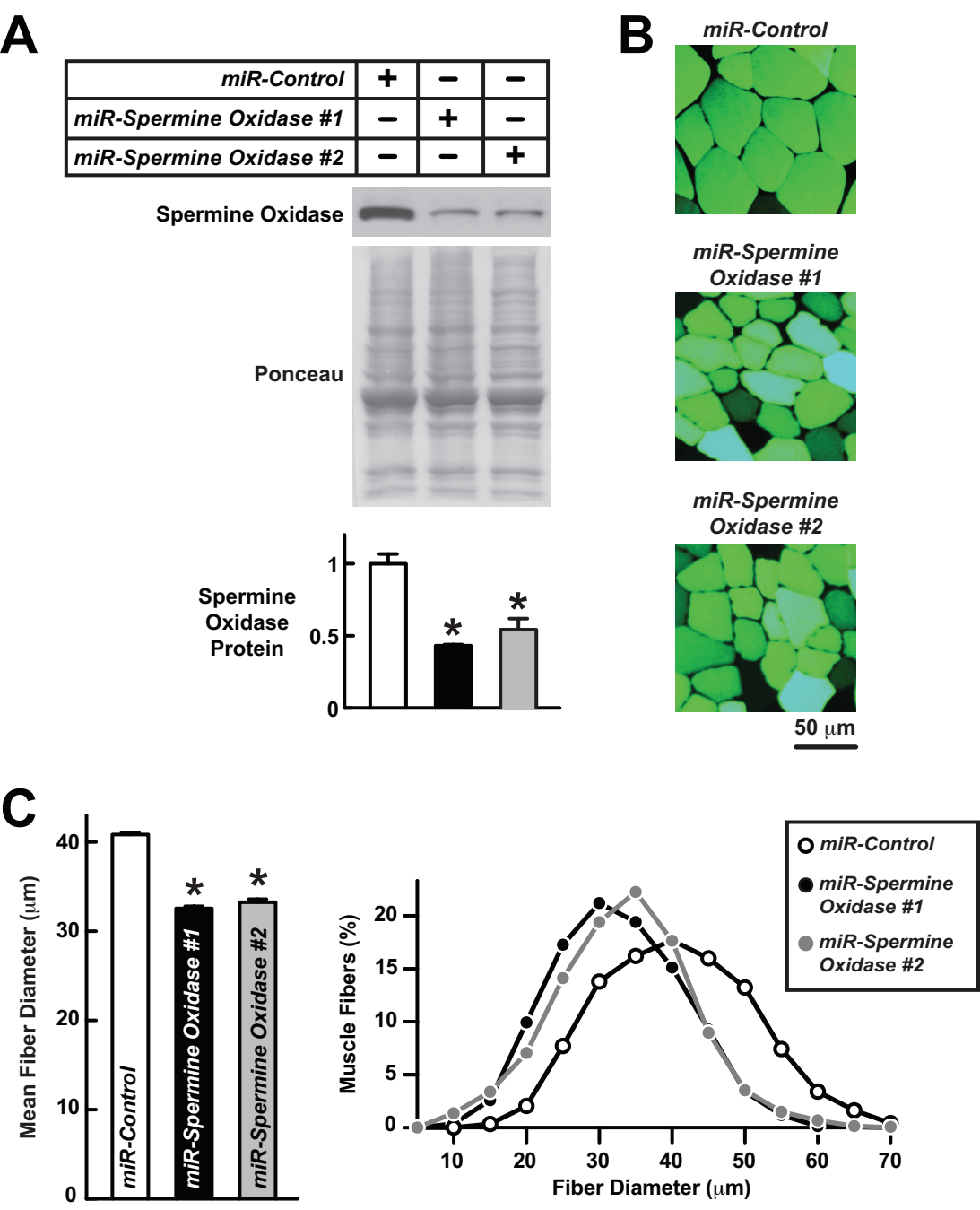
A
miR-Control + − −
miR-Spermine Oxidase #1 − + −
miR-Spermine Oxidase #2 − − +
Spermine Oxidase
Ponceau
Spermine Oxidase Protein
1
0.5
0
*
*
B
miR-Control
miR-Spermine Oxidase #1
miR-Spermine Oxidase #2
50 μm
C
Mean Fiber Diameter (μm)
40
30
20
10
0
miR-Control
miR-Spermine Oxidase #1
miR-Spermine Oxidase #2
*
*
Muscle Fibers (%)
20
15
10
5
0
10
20
30
40
50
60
70
Fiber Diameter (μm)
miR-Control
miR-Spermine Oxidase #1
miR-Spermine Oxidase #2

Figure 5

A Immobilized Muscles

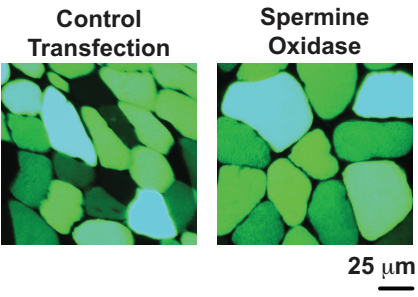

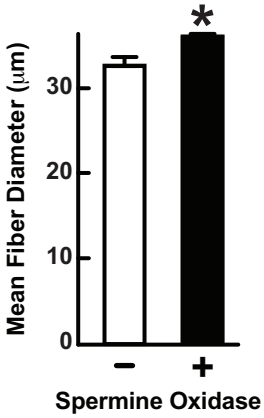

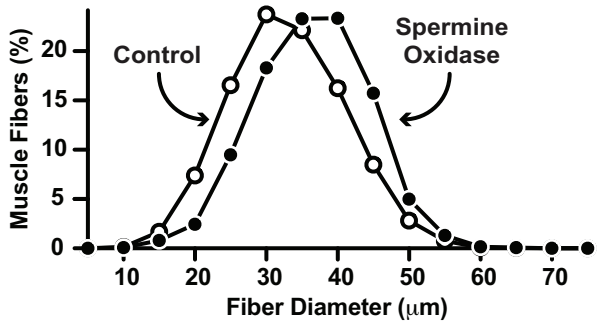

B Fasted Muscles

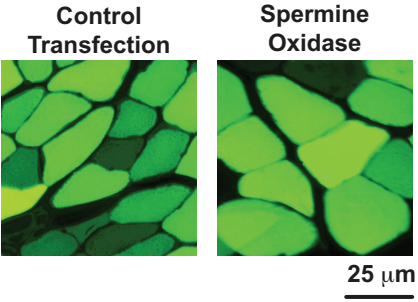

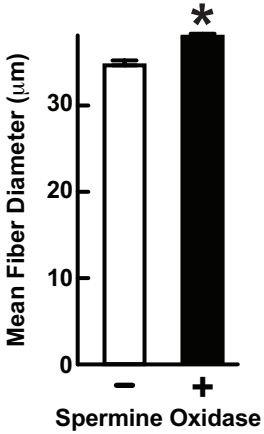

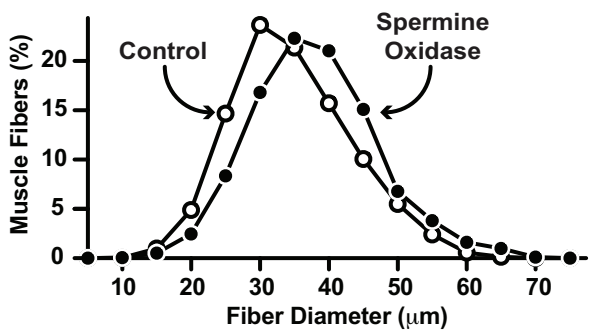

C Denervated Muscles

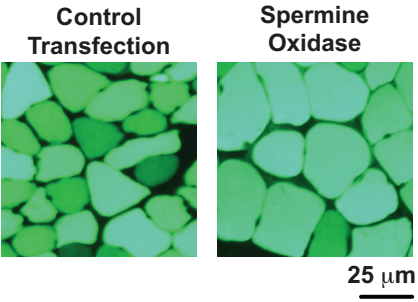

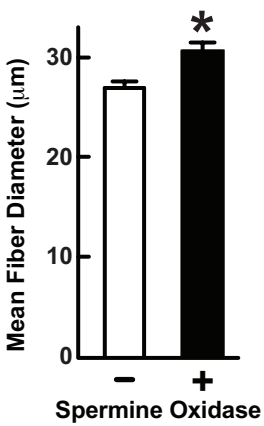

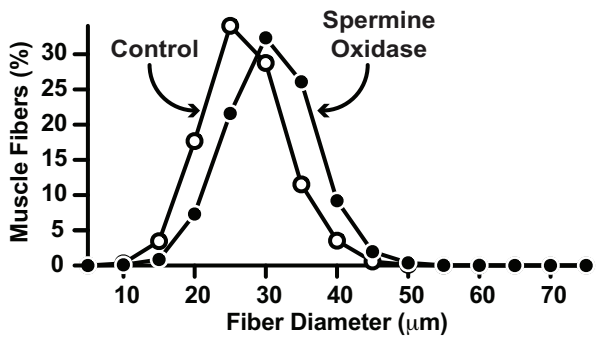

Figure 6

A **Skeletal Muscle mRNAs Most Reduced by p21 Overexpression**

Probe Rank	Log_2 Change	mRNA	Encoded Protein
1	**-1.44**	***Smox***	**Spermine Oxidase**
2	**-1.40**	***Smox***	**Spermine Oxidase**
3	**-1.26**	***Smox***	**Spermine Oxidase**
4	**-1.09**	***Smox***	**Spermine Oxidase**
5	-1.05	*Rcan2*	Regulator of Calcineurin 2
6	-1.04	*Knca7*	Potassium Voltage-Gated Channel, Shaker-Related Subfamily, Member 7
7	-1.01	*Cib2*	Calcium and Integrin Binding Family Member 2
8	-1.00	*Cib2*	Calcium and Integrin Binding Family Member 2
9	**-0.96**	***Smox***	**Spermine Oxidase**
10	-0.96	*Kcng4*	Potassium Voltage-Gated Channel, Subfamily G, Member 4

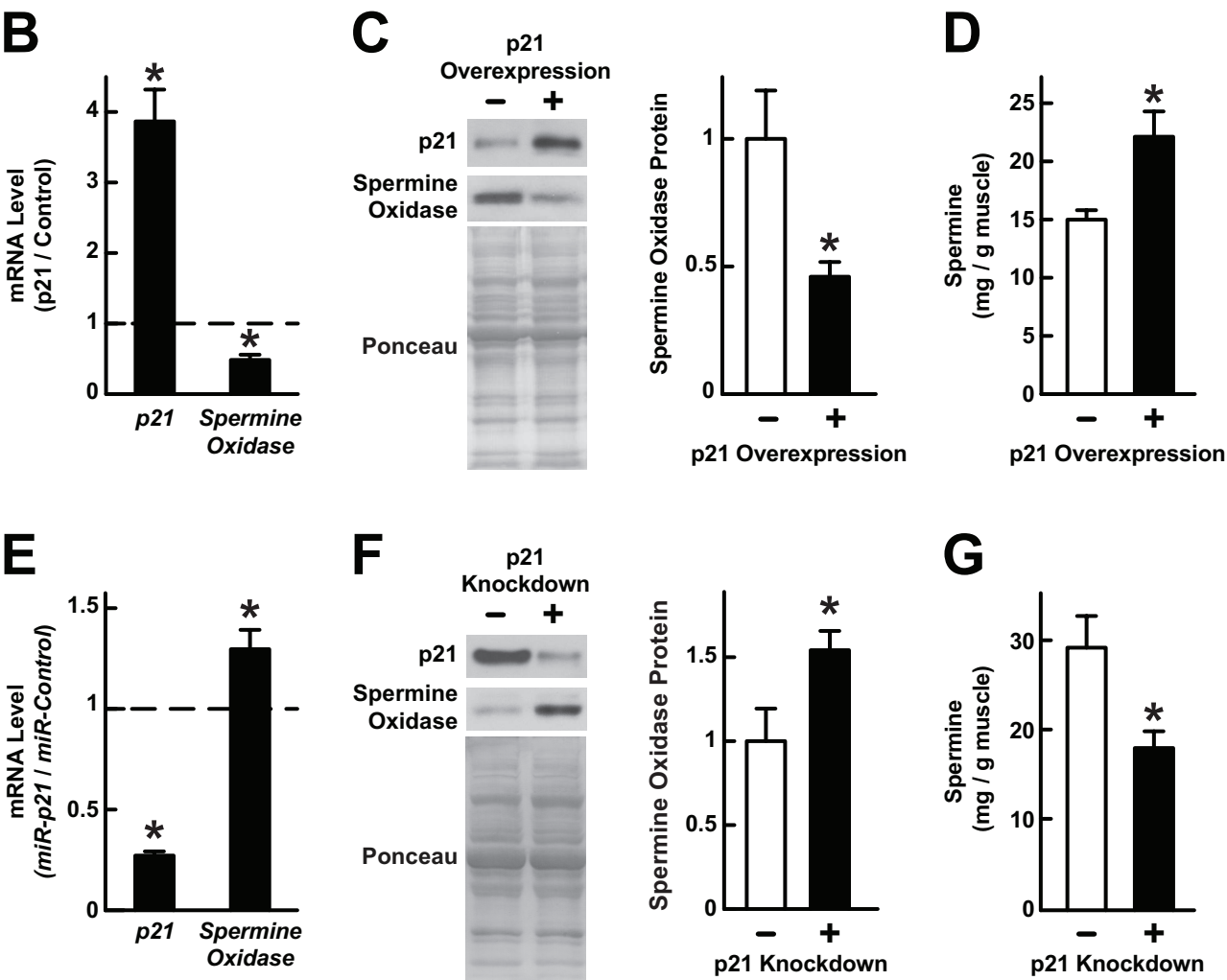

Figure 7

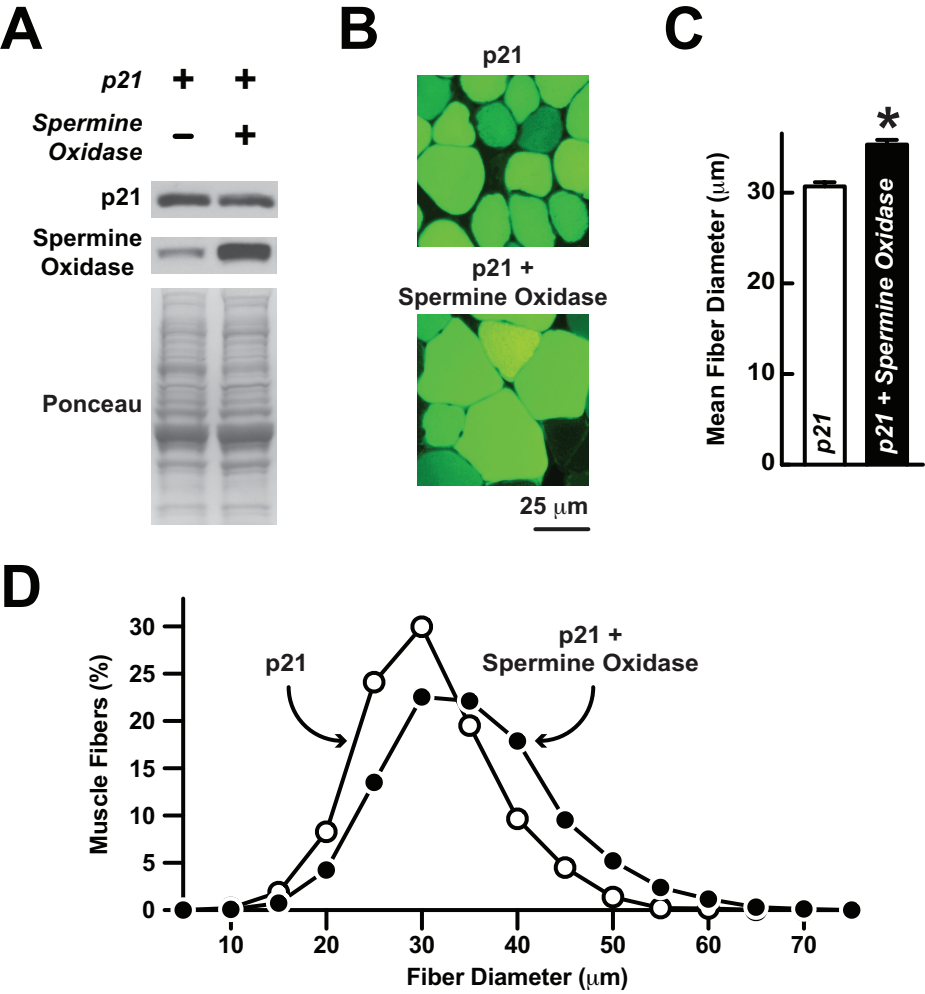
A
p21 + +
Spermine Oxidase − +
p21
Spermine Oxidase
Ponceau
B
p21
p21 +
Spermine Oxidase
25 μm
C
Mean Fiber Diameter (μm)
0
10
20
30
p21
p21 + Spermine Oxidase
*
D
Muscle Fibers (%)
0
5
10
15
20
25
30
p21
p21 +
Spermine Oxidase
10
20
30
40
50
60
70
Fiber Diameter (μm)

Figure 8

A

mRNAs Induced by Spermine Oxidase, and Repressed by Immobilization and p21

mRNA	Encoded Protein
Smox	Spermine Oxidase
Tspan8	Tetraspanin 8
Fbp2	Fructose Bisphosphatase 2
Magix	MAGI Family Member, X-linked
Ank	Progressive Ankylosis
Eepd1	Endonuclease/Exonuclease/Phosphatase Family Domain Containing 1
Tmem65	Transmembrane Protein 65
Igfals	Insulin-like Growth Factor Binding Protein, Acid Labile Subunit
Pcolce2	Procollagen C-endopeptidase Enhancer 2
Tmem204	Transmembrane Protein 204
Apbb2	Amyloid Beta (A4) Precursor Protein-binding, Family B, Member 2
Egln1	EGL Nine Homolog 1
Sun2	Sad1 and UNC84 Domain Containing 2
Maob	Monoamine Oxidase B
Mfn2	Mitofusin 2
P4ha1	Proline 4-hydroxylase, Alpha 1 Polypeptide
Ndufa3	NADH dehydrogenase (ubiquinone) 1 Alpha Subcomplex, 3
Atp5h	ATP Synthase, H+ Transporting, Mitochondrial F0 Complex, Subunit D
Ptp4a3	Protein Tyrosine Phosphatase 4a3
Clk3	CDC-like Kinase 3
Camk2a	Calcium/calmodulin-dependent Protein Kinase II Alpha

mRNAs Repressed by Spermine Oxidase, and Induced by Immobilization and p21

mRNA	Encoded Protein
Ncam1	Neural Cell Adhesion Molecule 1
Myog	Myogenin
Lrrn1	Leucine Rich Repeat Protein 1, Neuronal
Loxl1	Lysyl Oxidase-like 1
Maged1	Melanoma Antigen, Family D, 1
Hn1	Hematological and Neurological Expressed Sequence 1
Bhlhb9	Basic Helix-Loop-Helix Domain Containing, Class B9
Usp20	Ubiquitin Specific Peptidase 20
Ccdc134	Coiled-coil Domain Containing 134
Adamts2	A Disintegrin-like and Metallopeptidase with Thrombospondin Type 1 Motif, 2
Zfp36l1	Zinc Finger Protein 36, C3H Type-like 1
P4hb	Prolyl 4-hydroxylase, Beta Polypeptide
Med11	Mediator of RNA Polymerase II Transcription, Subunit 11 Homolog
Myod1	MyoD (Myogenic Differentiation 1)

B

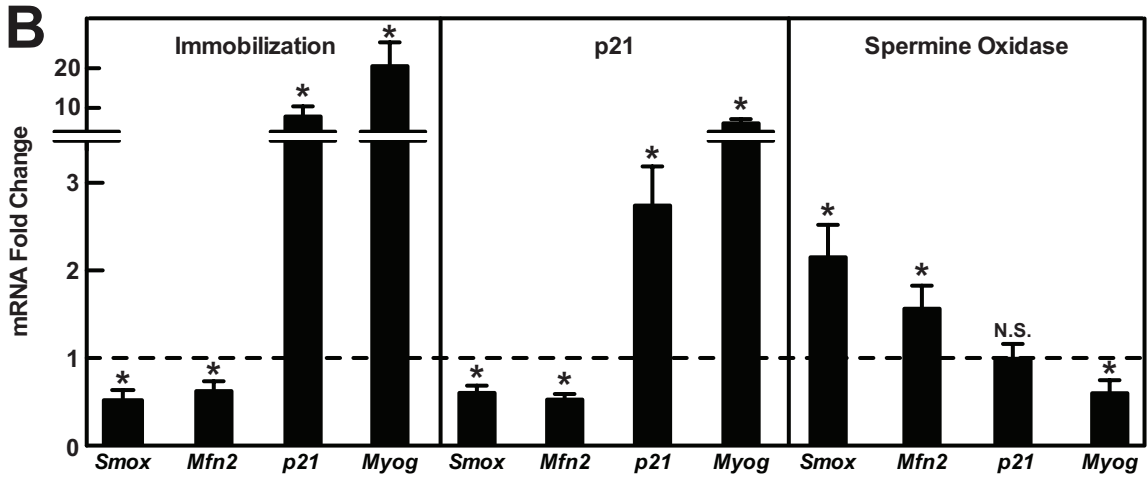

C

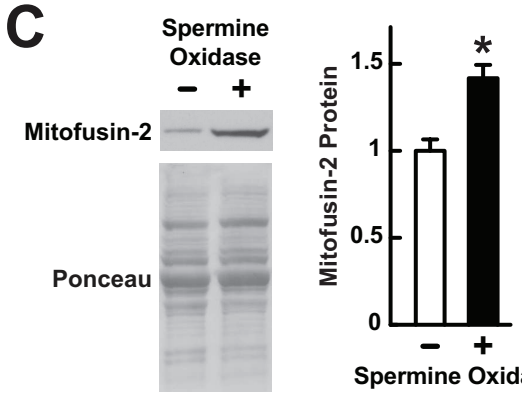

D

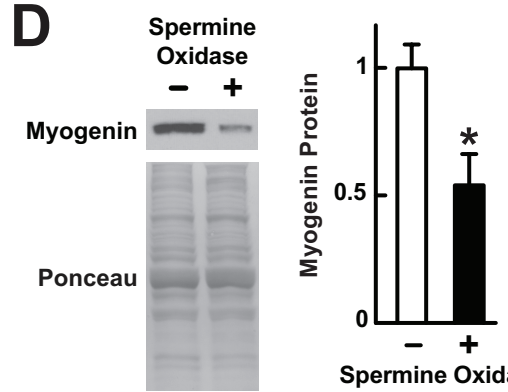

Figure 9

Gene Sets Induced by Spermine Oxidase, and Repressed by Immobilization and p21

Mitochondrial Biogenesis and Function
- Pyruvate Metabolism
- Oxidative Phosphorylation
- Respiratory Electron Transport
- TCA Cycle and Respiratory Electron Transport
- Citrate Cycle TCA Cycle
- Respiratory Electron Transport, ATP Synthesis by Chemiosmotic Coupling, and Heat Production by Uncoupling Proteins
- Mitochondrial Protein Import

Other Cellular Processes
- Peroxisome
- Voltage Gated Potassium Channels
- Phase 1 Functionalization of Compounds

Gene Sets Repressed by Spermine Oxidase, and Induced by Immobilization and p21

Inflammation
- Innate Immune System
- Interferon Alpha Beta Signaling
- Interferon Gamma Signaling
- RIG-I MDA5 Mediated Induction of IFN Alpha Beta Pathways
- Negative Regulators of RIG-I MDA5 Signaling
- Antigen Processing and Presentation
- GPVI Mediated Activation Cascade
- Chemokine Signaling Pathway
- Chemokine Receptors Bind Chemokines
- Natural Killer Mediated Cytotoxicity
- Toll Like Receptor Signaling Pathway
- Toll Receptor Cascades

Protein Metabolism
- Ribosome
- Peptide Chain Elongation
- Lysosome

Extracellular Matrix Remodeling
- Degradation of the Extracellular Matrix
- Glycosaminoglycan Degradation

Other Cellular Processes
- Cytosolic DNA Sensing Pathway
- Nonsense Mediated Decay Enhanced by the Exon Junction Complex
- Semaphorin Interactions
- Other Semaphorin Interactions

Figure 10

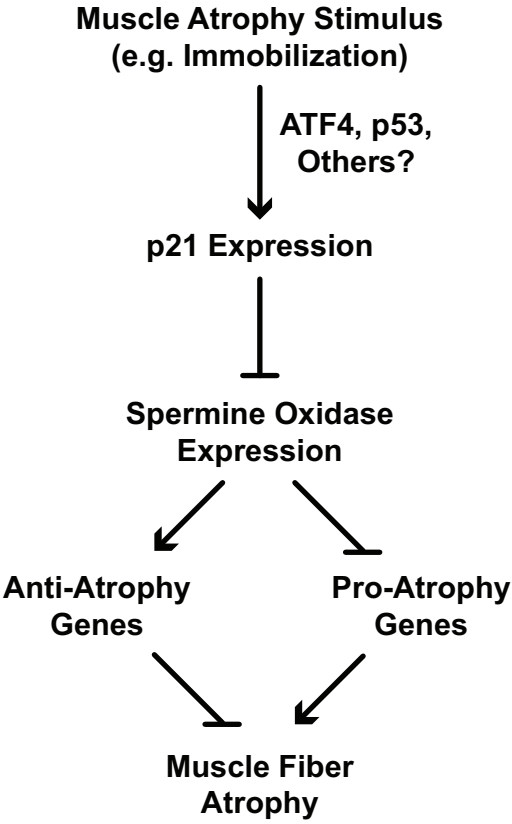
Muscle Atrophy Stimulus
(e.g. Immobilization)
ATF4, p53,
Others?
p21 Expression
Spermine Oxidase
Expression
Anti-Atrophy
Genes
Pro-Atrophy
Genes
Muscle Fiber
Atrophy